

# Radioactive source localization inside pipes using a long-range alpha detector<sup>\*</sup>

WU Xue-Mei(吴雪梅)<sup>1;2</sup> TUO Xian-Guo(庾先国)<sup>1;3;1)</sup> LI Zhe(李哲)<sup>2</sup> LIU Ming-Zhe(刘明哲)<sup>2</sup>  
 ZHANG Jin-Zhao(张金钊)<sup>2</sup> DONG Xiang-Long(董湘龙)<sup>2</sup> LI Ping-Chuan(李平川)<sup>2</sup>

<sup>1</sup> State Key Laboratory of Geohazard Prevention and Geoenvironment Protection,  
 Chengdu University of Technology, Chengdu 610059, China

<sup>2</sup> Provincial Key Laboratory of Applied Nuclear Techniques in Geosciences, Chengdu University of  
 Technology, Chengdu 610059, China

<sup>3</sup> Southwest University of Science and Technology, Mianyang 621010, Sichuan, China

**Abstract:** Long-range alpha detectors (LRADs) are attracting much attention in the decommissioning of nuclear facilities because of some problems in obtaining source positions on an interior surface during pipe decommissioning. By utilizing the characteristic that LRAD detects alphas by collecting air-driving ions, this article applies a method to localize the radioactive source by ions' fluid property. By obtaining the ion travel time and the airspeed distribution in the pipe, the source position can be determined. Thus this method overcomes the ion's lack of periodic characteristics. Experimental results indicate that this method can approximately localize the source inside the pipe. The calculation results are in good agreement with the experimental results.

**Key words:** LRAD, source position, ion travel time, airspeed, localization

**PACS:** 07.57.Kp, 29.40.-n, 85.25.Pb **DOI:** 10.1088/1674-1137/37/8/086201

## 1 Introduction

In contrast with traditional technologies, the long-range alpha detector (LRAD) has many advantages over traditional detectors. It detects alpha particles indirectly by collecting the ions produced by themselves. Thus, it can overcome the limitations of alpha particles, such as their short range and failure to penetrate facility walls [1].

Source activity detection and localization are demands of decommissioning nuclear facilities. So far, many countries have invested substantial money and labor to optimize and apply instruments for activity detection. Some researchers have extended to multi-parameter effects to build a nonlinear model that can forecast the readout of the instrument [2–9]. However, due to an ion's lack of periodic characteristics and many other unstable factors, the need for research on the localization of radioactive sources in nuclear facilities based on LRADs is not satisfied at present.

This paper presents a method to localize alpha particle sources inside pipes using an LRAD [10] without periodic characteristics. The method uses ion drift dis-

tance to establish the distance from source to detector. Based on the relationship between speed, time, and drift distance, it is important to obtain airspeed distribution in the pipe and ion travel time. Because ions are created from ambient air that is struck by alpha particles, their velocity is approximately equal to airspeed. However, pipe geometry and the uneven distribution of airspeed in a pipe make it hard to measure the airspeed distribution in a pipe with traditional tools. Therefore, FLUENT flow-modeling software is used to simulate the airspeed distribution inside the pipe [11, 12]. In addition, this paper applies computer-aided design (CAD) software to calculate ion travel time. Thus, source localization with LRAD-based pipe monitoring can finally be achieved.

## 2 The localization method

### 2.1 The experimental facility

This experimental facility mainly consists of two parts: an LRAD system and a testing part. The LRAD system contains five main parts: a sample detection part for complex surface monitoring (ion chamber and measurement chamber, shown in Fig. 1), an air-driver power,

Received 29 August 2012

<sup>\*</sup> Supported by National Science Fund for Distinguished Young Scholars of China (41025015), National Natural Science Foundation of China (41274108, 41274109), and Technological Innovation Research Team Foundation of Sichuan Province (2011JTD0013)

1) E-mail: tuoxg@cdu.edu.cn

2) E-mail: wxm1987\_com@sina.com

©2013 Chinese Physical Society and the Institute of High Energy Physics of the Chinese Academy of Sciences and the Institute of Modern Physics of the Chinese Academy of Sciences and IOP Publishing Ltd

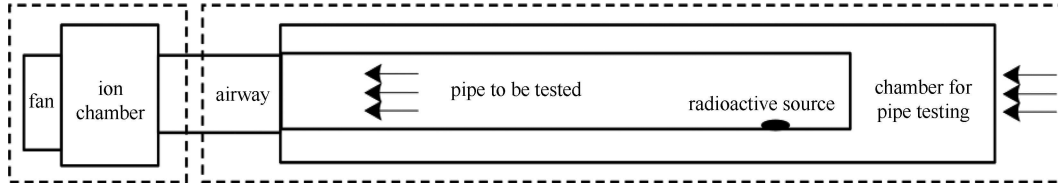


Fig. 1. The detection part of the LRAD system.

a detector power supply, a signal acquisition unit, and a processing unit [7–9]. The testing part comprises three stainless steel pipes, 152 cm in length with diameters of 43 mm, 48 mm, and 58 mm respectively. The dimensions of the ion chamber are 69 mm×106 mm×170 mm. The measurement chamber is a 164 cm long cylindrical cavity, with a diameter of 81 mm. The airway near the ion chamber is 20 cm long and 40 mm in diameter, while the distal air way is 11 cm high with a diameter of 35 mm.

By linking the signal-processing unit to a computer via a USB-to-RS232 serial cable, the system can obtain a series of real-time dynamic coordinates that describe readout change over time.

### 2.2 Localization based on ion travel time

Unlike electromagnetic wave methods that locate a source from a wave’s periodic characteristics, another reliable method is adopted to calculate the position of the source. Within the recombination time, ions created by alpha particles can be brought from the source into the ion chamber, which means that alpha particles can be detected by the LRAD wherever airflow can reach. Thus, the distance from the source to detector can be considered to be equal to the drift distance of ions. The movement of ions produced by alpha particles can be approximately regarded as the same as the air movement. Based on the relationship between drift distance, time, and velocity, this paper combines an LRAD system with

CAD and FLUENT software to establish ion travel time and airspeed distribution, and thus to calculate the drift distance of ions, which approximates the real position of the alpha source.

#### 2.2.1 Ion travel time

To calculate the drift distance of ions, it is important to establish their travel time,  $t$ , through the testing pipe. Here,  $t$  is defined as the time from the moment the software starts to the saturation point when most ions have reached the grid of the chamber.

However, a condition which restricts the measurement is that fan triggering time cannot be reflected in the output, and the saturation point cannot be presented during the experiment. Thus, ion travel time cannot be measured directly by any tool. It is therefore crucial to find a tool with a graphic function to present and measure the saturation point to obtain  $t$ .

This article uses CAD to draw a graph via its coordinates and also measure the length. As Fig. 2 shows, time from start to saturation point, marked  $t_2$ , can be presented by the deduction from a graph generated by CAD. A stopwatch is used to obtain time from start moment to fan triggering time, which is then entered into CAD, and measured as  $t_1$ . Thus, the two points that are needed to calculate  $t$  are determined from the graph. The last step is to use ‘dimlinear’ (a command of CAD) to measure the distance from  $t_1$  to  $t_2$ , and the software will automatically display this length. The length can

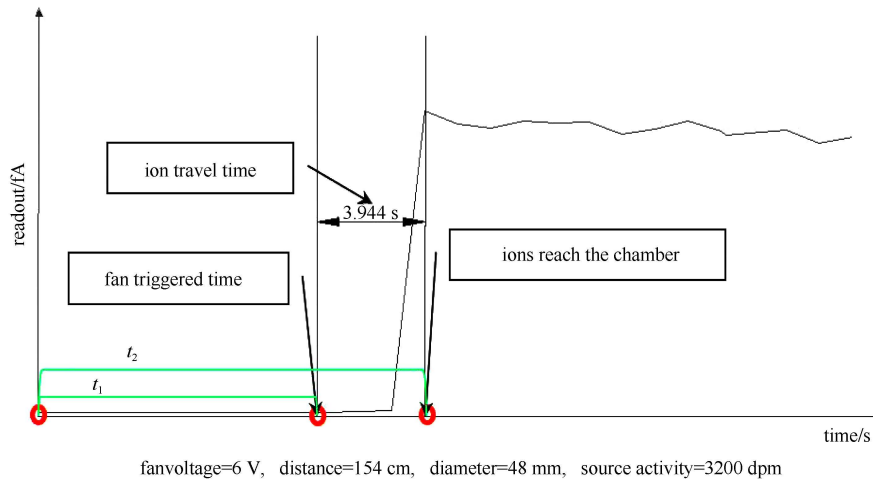


Fig. 2. The localization method based on ion travel time.

be converted into the difference between  $t_2$  and  $t_1$ .

### 2.2.2 Simulation of the spatial distribution of airspeed

To get the velocity field of the ions, FLUENT software is used to simulate the discrete coordinates on an LRAD plumbing mesh corresponding to the airspeed of the LRAD fluid model. These are then combined with the ion travel time localization method to analyze experimental results. With fluid analyzing, the effect of surface roughness on the velocity field is small enough to be ignored.

### 2.2.3 Localization based on ion travel time

For ion travel time, by using method shown in Fig. 2, due to some practical operating limitations, the real time from fan triggering to saturation point cannot actually be recorded. When using a dimlinear command to measure difference between  $t_1$  and  $t_2$ , CAD will automatically display  $t$ .

On the other hand, FLUENT simulates airspeed distribution for the whole model. As the distance from source to detector is considered to be equal to the ion drift distance, data exported from FLUENT should be consistent with the ion direction. The  $x$ -coordinate data, whose direction is consistent to source-to-detector direction, are thus chosen for further calculation. However, as each velocity in the simulation corresponds to an  $x$ -coordinate,  $t$  cannot be directly multiplied by velocity to calculate the source position. Thus these distances are defined as differential drift distance  $dx$ , and velocity as  $v_x$ . The deduced time interval of an ion traveling from one coordinate to an adjacent one is then  $dt=dx/v_x$ . After accumulating these time intervals one by one, the theoretical ion travel time is defined as  $t'=\sum t$ . The final localization result is determined by finding the corresponding  $x$ -coordinate where accumulated time  $t'$  equals  $t$  as measured by the localization method shown in Fig. 2.

## 3 Results and discussion

### 3.1 Ion static distribution

Before the fan is triggered, the ion distribution should be considered. As ions are generated by alphas, this article analyzes it as follows.

Without a fan, the stretch of alphas depends on its range. Following is the formula of alpha range in air:

$$R=0.309E^{3/2},$$

$R$  is alpha range in air,  $E$  is alpha energy. The alpha energy emitted by  $^{239}\text{Pu}$  is 5.115 MeV. Substituting it into the formula, the theoretical alpha range is calculated as 3.57 cm. Thus, the alpha distribution is generally like a ball with 3.57 cm radius, surrounding the source. Fig. 3 shows the distribution.

However, it is not that easy to obtain a static distri-

bution of ions. After an alpha collides with one molecule of ambient air, there will be two kinds of particles, positive ions and electrons. Each pair costs 35 eV. For an electron, the range is limited by its energy (less than 35 eV), while a positive ion is also affected by its weight.

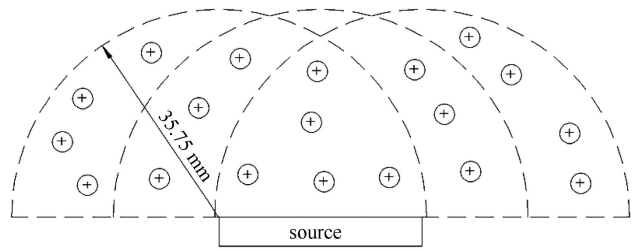


Fig. 3. The alpha static distribution.

In order to obtain a more accurate range, an experiment was carried out in three steps. The first step was background measurement in a pipe of 48 mm in diameter. Then four sources were put at the near-end of the testing pipe (also at the airway nozzle in front of the detector) respectively, and performed without airflow. The last step was to be done with airspeed of 0.639 m/s for four sources. Table 1 shows the result.

From Table 1, it is obvious that the close range measuring results are almost the same as the background ones, while the results with airspeed are significantly larger. That is to say, ions without airflow cannot reach the ion chamber. Thus, it is deduced that the ion range is less than that of the airway, which is measured to be 10 cm.

Table 1. Experimental results (fA).

source activity/Bq	airspeed/(m·s <sup>-1</sup> )		background/fA
	0	0.639	
24.05	83.90	177.00	82.87
182.50	80.53	565.66	82.87
523.33	83.61	1584.54	82.87
3200	81.51	12767.64	82.87

As alpha decay was in a dynamic balance, the ions arrived at the ion chamber with a uniform flow. The saturation point was considered as the highest density of the first flow, corresponding to the center of the source profile. That is, ion distribution has little effect on the measurement results. So we ignore the effect of ion distribution here.

### 3.2 Ion travel time $t$

This experiment was tested with a calibrated  $^{239}\text{Pu}$  alpha resource with an activity of 523.33 Bq, and the ion travel time was obtained using the apparatus shown in Fig. 2. The experiment was repeated five times for each condition. Table 2 shows the theoretical ion travel time under different conditions. The pipe diameter in this experiment was 48 mm and the length was 152 cm.

To test the availability of above-mentioned theory, three different airspeeds measured at the distal end of the pipe were chosen, 0.639 m/s, 1.473 m/s, and 2.254 m/s, respectively, working at two different source-detector distances, 0.94 m and 1.54 m.

Table 2. The ion travel time of source at 0.94 m and 1.54 m under three airspeeds (s).

source-detector distance/m	airspeed/(m·s <sup>-1</sup> )		
	0.639	1.473	2.254
0.94	4.06±0.39	2.36±0.24	1.41±0.17
1.54	6.80±0.08	3.88±0.25	2.71±0.24

Table 2 shows ion travel time under each condition plus or minus the standard error of the five results. When ion velocity is slow enough, the results clearly indicate a negative linear relationship between ion travel time and airspeed, which is broadly in line with the principle  $dt=dx/v_x$ . At the same time, the standard error of each evaluated ion travel time shown is sufficiently small.

### 3.3 Airspeed spatial distribution simulated by FLUENT

The computational fluid dynamics numerical simulation for the LRAD system fluid model first applies Gambit preprocessing software to build and mesh the model to digitalize the space into a series of coordinates. Then the input ‘.msh’ file is exported from Gambit into the FLUENT solver to simulate airspeed distributions under different conditions. According to the airspeeds of “-x” direction  $v_x$  and distance coordinates, source positions can be calculated when combined with ion travel time.

The process starts with model building by using Gambit software. As Fig. 1 shows, the specifications of the model are based on those presented in Section 2.1. Considering the complexity of the geometry, an unstruc-

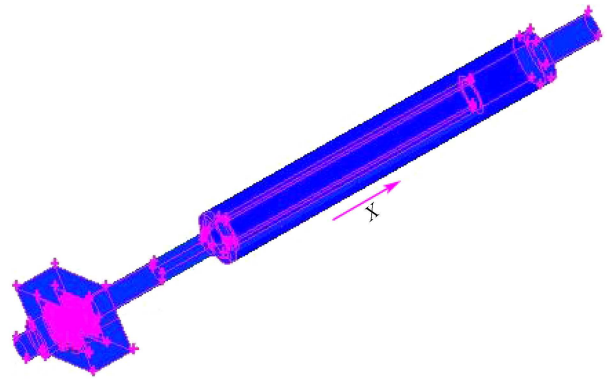


Fig. 4. (color online) The meshed LRAD experimental model.

tured grid was adopted for this equipment. Fig. 4 shows the meshed LRAD experimental model.

The preliminary work before FLUENT solving required that boundary conditions were defined after being meshed. According to the known conditions, the boundary conditions were confirmed as velocity-inlet and outflow. The velocity-inlet was defined as the nozzle of the distal air tube, while the outflow was the nozzle in front of the ion chamber. The model being proven to be turbulence flow, the  $k-\epsilon$  turbulence model was adopted for model simulation, with the threshold for convergence of the variable residual set at  $10^{-5}$ . During the simulation, the velocity-inlet was set at 0.639 m/s, 1.473 m/s and 2.254 m/s, and the thermodynamic temperature at 288 K. Other values were kept at default values.

### 3.4 Localization of the source inside the pipe

Combining ion travel time generated by CAD with coordinate-airspeed distribution generated by FLUENT, the localization results were derived under six different conditions. The method is shown in Fig. 5 and the results are shown in Table 3.

x-coordinate	x-velocity	coordinates spacing	space time of coordinates	cumulative time
$x_1$	$v_1$	$dx$		$dt$
$x_2$	$v_2$	$x_2-x_1$	$(x_2-x_1)/v_1$	$t_1=(x_2-x_1)/v_1$
$x_3$	$v_3$	$x_3-x_2$	$(x_3-x_2)/v_2$	$t_2=(x_3-x_2)/v_2+t_1$
$\vdots$	$\vdots$	$\vdots$	$\vdots$ when $t_n=t$ (CAD calculated) $\vdots$	
$x_{n-1}$	$v_{n-1}$	$x_{n-1}-x_{n-2}$	$(x_{n-1}-x_{n-2})/v_{n-2}$	$t_{n-1}=(x_{n-1}-x_{n-2})/v_{n-2}+t_{n-2}$
$x_n$	$v_n$	$x_n-x_{n-1}$	$(x_n-x_{n-1})/v_{n-1}$	$t_n=(x_n-x_{n-1})/v_{n-1}+t_{n-1}$
$x_{n+1}$	$v_{n+1}$	$x_{n+1}-x_n$	$(x_{n+1}-x_n)/v_n$	$t_{n+1}=(x_{n+1}-x_n)/v_n+t_n$

Fig. 5. The localization principle based on the FLUENT export data.

Table 3. Localizations for source at 0.94 m and 1.54 m at three airspeeds.

airspeed/(m·s <sup>-1</sup> )	0.94 m		1.54 m	
	estimated position/m	relative error/%	estimated position /m	relative error/%
0.639	1.023	8.8	1.559	1.25
1.473	0.970	3.2	1.515	1.65
2.254	1.059	12.7	1.478	4.00

By obtaining distance  $ds$  between adjacent coordinates, time interval  $dt$  could thus be conveniently calculated, as shown in Fig. 5. When  $t_n = t$ , a corresponding  $X_n$  was taken as the localization result. Table 2 shows the calculated source localizations at 0.94 m and 1.54 m for three airspeeds. The calculated localizations of two positions are approximate to the real position. Although  $x$ -velocity turned out to be negative, this did not influence the results because the  $x$ -coordinate direction was simply defined as being opposite to ion direction.

Table 3 shows that all of the calculated localizations are significantly approximate to real positions. In addition, the maximum relative simulation error is less than 13%, and others are less than 10%. Thus, this method of source localization based on LRAD monitoring of pipe interiors can be considered reliable. Additionally, the relative error at 1.473 m/s is smaller than the other two airspeeds, so this airspeed can be taken as the optimal condition for this method. However, the relative errors of the source are greater at 0.94 m than at 1.54 m. It is probably caused by a sudden change of pipe diameter.

Further work is required to account for this.

## 4 Conclusions

The use of CAD and FLUENT software to find ion travel time  $t$  and airspeed distribution helps to obtain localization results that approach real positions. Hence, it can be concluded that the use of this LRAD-based source localization method on pipe monitoring is effective and reliable. Adoption of this method during site pipe decommissioning could not only assist in finding source position nondestructively, but also in overcoming the nonlinearity effect of activity measurement. However, errors still exist. From Table 3, it is obvious that the source location at 94 cm with airspeed of 2.254 m/s obtains the largest relative error. In addition, error at 94 cm is greater than that at 154 cm. Further work is needed to reduce time errors, which may be caused by signal transmission delay and operational errors, and further study of aerodynamics is needed to find a reliable process to optimize the FLUENT simulation.

## References

- 1 WANG G, FU K, YAO C S et al. Nucl. Instrum. Methods A, 2012, **663**: 10
- 2 MacArthur D W, Allander K S, Bounds J A et al. Los Alamos National Lab., NM LA-12199-MS. 1991
- 3 Johnson J D, Allander K S, Bounds J A et al. Nucl. Instrum. Methods A, 1994, **353**: 486
- 4 Rojas S P, Rawool-Sullivan M W et al. Waste Management '95 Conference Tucson, LA-UR-95-174. 1995
- 5 Whitley C R, Adams J R, Bounds J A et al. New Mexico Conference on the Environment, Albuquerque LA-UR-96-578. 1996
- 6 Rawool-Sullivan M W, Conaway J G, MacArthur D W et al. Los Alamos National Laboratory, LA-13063-MS. 1996
- 7 TUO Xian-Guo, LI Zhe, MU Ke-Liang et al. Journal of Nuclear Science and Technology, 2008, supplement 5. 282
- 8 HUANG Lian-Mei. Research on Key-parameter Experiments and PLS-BP Correction Approach: LRAD Measurements Inside Pipes (Master Thesis). Chengdu: Chengdu University of Technology, 2011 (in Chinese)
- 9 WU Xue-Mei, TUO Xian-Guo, LI Zhe et al. Nuclear Techniques, 2012, **35**: 369
- 10 Bouhadef B. Nucl. Instrum. Methods A, 2009, **604**: S230
- 11 WU Yan, GAO Jia-Rong, HU Yong-Peng. New Technology & New Process, 2010, **10**: 33
- 12 JIANG Xiao-Fang, CAO Xi-Jing, SI Zhen-Peng. Process Equipment & Piping, 2009, **46**: 0046